NATIONAL BUREAU OF STANDARDS REPORT

7367

THERMAL CONDUCTIVITY OF SEMICONDUCTIVE SOLIDS;
METHOD FOR STEADY-STATE MEASUREMENTS ON
SMALL DISK REFERENCE SAMPLES

Technical Progress Report
for Period
July 1 to September 30, 1961

by

D. R. Flynn

Report to the
Bureau of Ships
Department of the Navy
Washington, D. C.

NBS

U. S. DEPARTMENT OF COMMERCE

NATIONAL BUREAU OF STANDARDS

THE NATIONAL BUREAU OF STANDARDS

Functions and Activities

The functions of the National Bureau of Standards are set forth in the Act of Congress, March 3, 1901, as amended by Congress in Public Law 619, 1950. These include the development and maintenance of the national standards of measurement and the provision of means and methods for making measurements consistent with these standards; the determination of physical constants and properties of materials; the development of methods and instruments for testing materials, devices, and structures; advisory services to government agencies on scientific and technical problems; invention and development of devices to serve special needs of the Government; and the development of standard practices, codes, and specifications. The work includes basic and applied research, development, engineering, instrumentation, testing, evaluation, calibration services, and various consultation and information services. Research projects are also performed for other government agencies when the work relates to and supplements the basic program of the Bureau or when the Bureau's unique competence is required. The scope of activities is suggested by the listing of divisions and sections on the inside of the back cover.

Publications

The results of the Bureau's research are published either in the Bureau's own series of publications or in the journals of professional and scientific societies. The Bureau itself publishes three periodicals available from the Government Printing Office: The Journal of Research, published in four separate sections, presents complete scientific and technical papers; the Technical News Bulletin presents summary and preliminary reports on work in progress; and Basic Radio Propagation Predictions provides data for determining the best frequencies to use for radio communications throughout the world. There are also five series of nonperiodical publications: Monographs, Applied Mathematics Series, Handbooks, Miscellaneous Publications, and Technical Notes.

A complete listing of the Bureau's publications can be found in National Bureau of Standards Circular 460, Publications of the National Bureau of Standards, 1901 to June 1947 ($1.25), and the Supplement to National Bureau of Standards Circular 460, July 1947 to June 1957 ($1.50), and Miscellaneous Publication 240, July 1957 to June 1960 (Includes Titles of Papers Published in Outside Journals 1950 to 1959) ($2.25); available from the Superintendent of Documents, Government Printing Office, Washington 25, D. C.

NATIONAL BUREAU OF STANDARDS REPORT

NBS PROJECT

1006-20-10461 ,November 14, 1961

NBS REPORT

7367

THERMAL CONDUCTIVITY OF SEMICONDUCTIVE SOLIDS;
METHOD FOR STEADY-STATE MEASUREMENTS ON
SMALL DISK REFERENCE SAMPLES

Technical Progress Report
for period
July 1 to September 30, 1961

by

D. R. Flynn
Heat Transfer Section
Building Research Division

Report to the
Bureau of Ships
Department of the Navy
Washington, D. C.

INDEX NO. S-R007 12 01, Task No. 800
(BuShips 1700S-696-61). Code 342B

$\langle NBS \rangle$

U. S. DEPARTMENT OF COMMERCE
NATIONAL BUREAU OF STANDARDS

Thermal Conductivity of Semiconductive Solids;
Method for Steady-State Measurements on
Small Disk Reference Samples

by

D. R. Flynn

1. ABSTRACT

Thermal conductivity measurements were conducted
over the temperature range 200° to 1200°C on the bar of
60% platinum-40% rhodium alloy from which the hot and cool
contacting bars of the high-temperature apparatus are to be
fashioned. The tentative results, not yet corrected for
individual thermocouple variations, plot smoothly from
0.57 w/cm-C at 200°C to 0.79 w/cm-C at 1200°C. A paper
"Thermal Guarding of Cut-Bar Apparatus," which was presented
at the Invitational Conference on Thermal Conductivity
Methods held at Battelle Memorial Institute, Columbus, Ohio,
on October 26-28, 1961, is reproduced following the main
body of this report.

2. STATEMENT OF PURPOSE

To develop a method and apparatus for steady-state
thermal conductivity measurements at temperatures to 800°C
and above, and suitable for solids in the form of small
specimens (1/2-in. by 1-in. diameter disks), with the
objective of providing samples for use by other laboratories
as thermal conductivity reference specimens in connection
with their measurements on solid semiconductors.

3. WORK PERFORMED IN REPORTING PERIOD
(July 1 to September 30, 1961)

During this quarter additional measurements of the
thermal conductivity of the 60% platinum-40% rhodium alloy
were completed, using the high temperature model of the
absolute cut-bar apparatus. (For a description of this
equipment, see NBS Report 7323.)

In the course of these measurements, it was found that
to maintain the desired temperature distributions along the
alumina guard cylinder, two additional heaters of platinum-
20% rhodium wire were required near the ends of the cylinder.
These heaters, shown in the schematic diagram of the apparatus
(Fig. 1), are controlled by variable voltage transformers to
minimize end heat losses from the central portion of the guard
cylinder.

The thermal conductivity of the 60% platinum-40% rhodium alloy was remeasured over the temperature range 200° to 1200°C. The alloy was supported between the alumina tube below and the alumina rod above. The thermal insulation used throughout the apparatus was alumina powder. The power generated in the specimen heater was determined by current and potential drop measurements, using a calibrated volt box and shunt box in conjunction with a precision potentiometer.

The temperature distribution along the platinum-rhodium bar was determined by means of four butt-welded platinum: platinum-10% rhodium thermocouples, fabricated from calibrated reference grade wire, pressed into four 0.3 mm grooves in the convex surface of the bar. Each of the four specimen thermocouples could be read against an ice junction, so that temperature gradients could be determined by difference.

When the 60% platinum-40% rhodium alloy bar was purchased, a 0.5 mm wire was drawn by the manufacturer from the same material. A thermocouple, fabricated from a length of this wire and a length of 0.38 mm reference grade platinum wire, was calibrated by the NBS Pyrometry Laboratory over the temperature range 0°-1100°C. Using this calibration curve, the thermoelectric power of the platinum-40% rhodium alloy against platinum and against platinum-10% rhodium was derived.

The insulated room-temperature zone box was wired to enable determination of the emf developed between similar leads of different thermocouples. The emf was measured between the platinum wires of the lower two junctions, the platinum wires of the upper two junctions, the platinum-10% rhodium wires of the lower two junctions, and the platinum-10% rhodium wires of the upper two junctions. Thus, the 60% platinum-40% rhodium bar served as the central portion of four differential thermocouples.

Thermal conductivity measurements were made in increasing order of temperature from 200° to 1200°C at 200 deg C intervals, and then in decreasing order of temperature at 800° and 400°C. Each conductivity determination involved two tests. First, an "isothermal" test, in which there was no power input to the specimen heater, was made to determine variations between specimen thermocouples. This test was followed by a "gradient" test with sufficient power input to the specimen heater to maintain a longitudinal temperature gradient in the specimen of about 2 deg C/cm. In all of the tests, the guards were adjusted so that there was very little net heat exchange between the specimen bar assembly and the surrounding insulation.

The results of the gradient tests are plotted in Figure 2. The conductivities shown are computed from "raw" data only. That is, the temperature readings from the gradient

tests have not been corrected for the thermocouple variations determined by the isothermal tests. These corrections have been postponed pending installation of improved digital computer facilities at NBS.

The solid symbols shown in Figure 2 represent measurements made with temperatures increased, and open symbols those made with temperatures decreased. Thermal conductivity values indicated represent the average of two conductivities: one computed using the temperature difference between the lower two specimen thermocouples and the other that between the upper two specimen thermocouples. The circles (solid and open) were obtained using temperature gradients as determined by differences between the platinum:platinum-10% rhodium thermocouples read against an ice junction. The triangles (solid and open) were obtained using temperature gradients as determined by the platinum:platinum-40% rhodium:platinum differential thermocouples in which the specimen was the central leg.

The solid line shown in Figure 2 is the least-mean-squares quadratic through all of the points shown. The dashed lines above and below the solid line bound the region plus and minus 5 percent of the solid line. The data shown are to be considered tentative, since corrections have not been made for variations between thermocouples. When these corrections are made, the data should be significantly smoother.

4. FUTURE ACTIVITIES

Measurements will begin in a few weeks on a specimen of the nickel-chrome alloy that was measured in the modified prototype absolute cut-bar apparatus. This material has also been measured in two models of the NBS metals apparatus and in the NBS steam calorimeter apparatus. Its conductivity is believed to be well known (±2 percent) over the temperature range -150° to 1000°C and hence this material should be quite suitable for confirming the accuracy of the high temperature absolute cut-bar apparatus.

A 1/2-inch by 1-inch diameter disk of Pyroceram 9606 is currently being optically polished. This specimen will be ultrasonically cleaned and the flat surfaces coated with vapor-deposited platinum. Thermocouples will be affixed in small grooves cut in the convex surface of the specimen to enable determination of the temperature gradient in the specimen. A large specimen of the same material has been prepared for measurement in the NBS metals apparatus. These independent measurements in the absolute cut-bar apparatus and the metals apparatus will provide a cross-check on a material of conductivity similar to that of many thermoelectric materials of interest and will assist in determining the suitability of this material for thermal conductivity reference purposes.

5. USE OF A REFERENCE MATERIAL

The ultimate objective of this research is the provision,
for use by other laboratories, of suitable thermal conduc-
tivity reference specimens. Of equal importance, it is felt,
is the proper use of such standards.

The problems encountered in the design and operation of
the absolute cut-bar apparatus have pointed out some of the
difficulties arising in measurements of this type on small
samples. The two most serious difficulties are due to the
thermal resistances at the contacting surfaces of the specimen
and the extraneous exchange of heat with the surrounding insu-
lation. In order to avoid the problem of attempting to measure
contact resistance, it is recommended that thermocouples be
placed in the specimen not too near its contact surfaces. In
order to evaluate heat exchanges with the insulation, a mathe-
matical analysis was made. The general form of this analysis
was presented in Appendix A of NBS Report 7135 (April 28,
1961).

A detailed analysis of heat flow in the insulation of a
simplified cut-bar apparatus was presented by this author at
the Invitational Conference on Thermal Conductivity Methods
held at Battelle Memorial Institute, Columbus, Ohio, on
October 26-28, 1961. In view of the similarity of this analy-
sis to that used for the NBS absolute cut-bar apparatus, this
paper "Thermal Guarding of Cut-Bar Apparatus" is reproduced
at the end of this report.

Many laboratories are currently utilizing various forms
of a comparative cut-bar apparatus for their thermal conduc-
tivity measurements. A typical example would be the apparatus
of Francl and Kingery[1]. As has been pointed out, shunting
heat flows through the insulation are a serious problem in an
apparatus of this type. While these heat flows are evaluated
analytically in this laboratory, it is realized that many
laboratories will not find it convenient to resort to a digital
computer for evaluation of their particular apparatus.

The effects of these unwanted heat flows can be avoided
by means of a suitable calibration if suitable thermal conduc-
tivity reference specimens can be made available. The best
use of these reference specimens is summed up in another paper
presented at the above-mentioned conference. In his paper
"Current NBS Steady-State Thermal Conductivity Methods," H. E.
Robinson, Chief of the NBS Heat Transfer Section, concluded
by saying:

---

1. J. Am. Ceram. Soc. 37 [2] 80-84 (1954).

"The idea of a thermal conductivity reference standard is manifest. Nevertheless, such standards involve other problems than merely those of selecting suitable materials and determining their conductivity as accurately as possible.

"For example, the best use of a reference material is to use it as a substitute specimen, as is done for instance in precise determinations of electrical resistance. When the reference is used in this way in a particular apparatus, it is presumably subject to the same unwanted heat flows, resulting from what might be termed the accessory conditions of the apparatus, as would be a test of specimen of equal conductivity. If the reference is thus used to calibrate a metering device of some sort, as it would be in a comparative type of testing apparatus, the calibration of the meter would inherently contain the effects of these perturbations. This consideration is of special importance in the case of heat flow measuring equipment, because there is no perfect thermal insulation or guarding to eliminate unwanted heat flows. Such use of the reference as a substitute specimen carries with it, however, the strict requirement that the accessory conditions of the apparatus be duplicable in ordinary tests, as in the calibrating tests. Thus, in this sense, the best use of a reference standard involves the design of the apparatus to be calibrated with it, in regard to the precision with which the accessory conditions can be controlled and duplicated.

"As an illustration, it would not be the best use of a reference material of known conductivity to employ it as the heat flow meters in a series arrangement such as meter-specimen-meter. The better use would be to employ for the metering bodies some suitable material, and obtain a calibration for them by using the reference in place of the speci-men. If reference substitute specimens covering a range of conductivities were used, and accessory conditions were ade-quately reproduced, it is probable that test measurements on unknown specimens of conductivities within the range covered by the references could be made with results not seriously inferior in absolute value to those of the reference speci-mens......"

THRUST

COOLANT →

GUARD CYLINDER

HEATERS

COLD BAR

SPECIMEN

HOT BAR

INSULATION

NOTES:

X   denotes the position
     of a thermocouple
     junction

Δ   denotes the position
     of a differential
     thermocouple junction

COOLANT
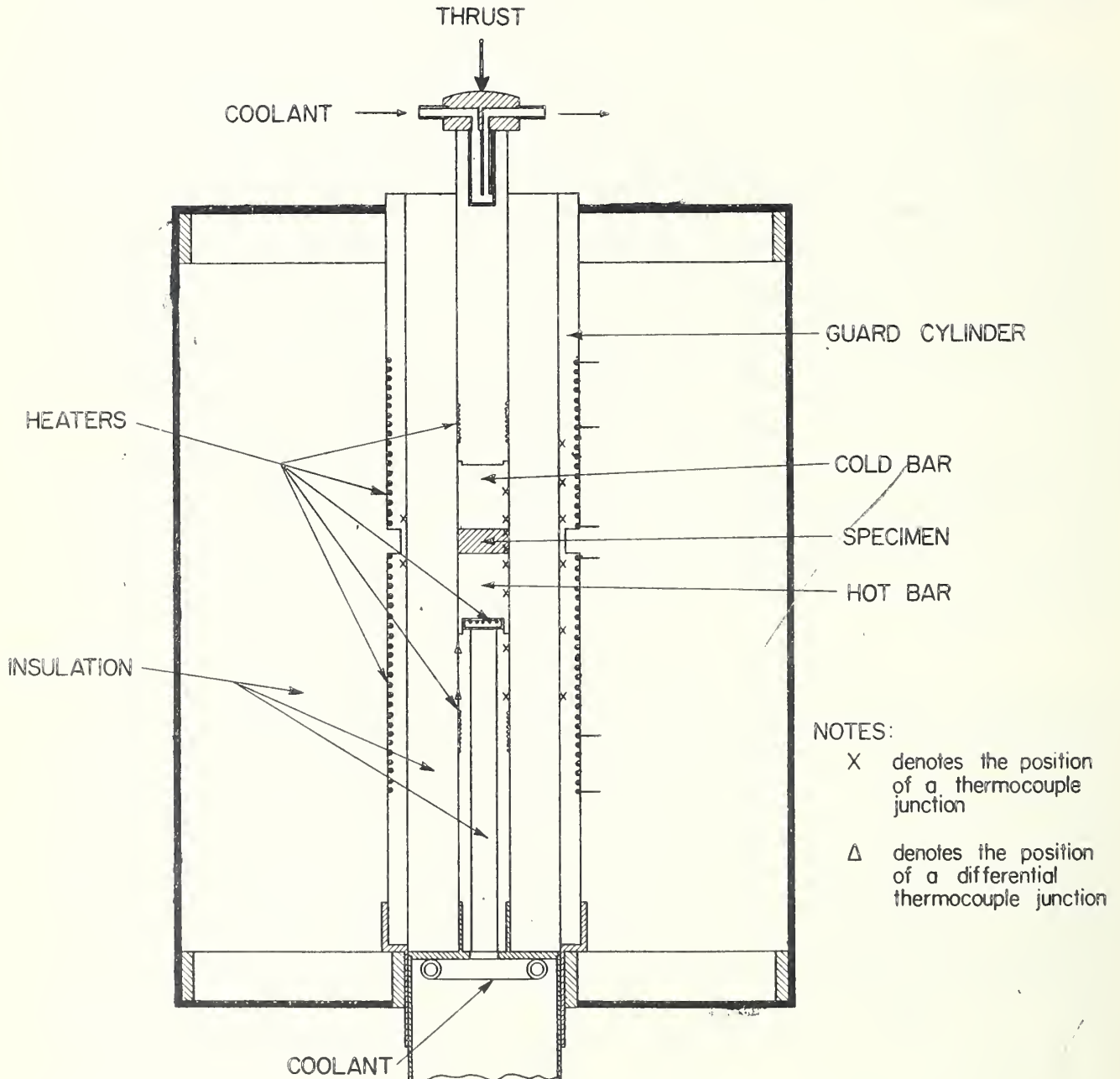
Figure 1.   High temperature absolute cut-bar apparatus for
determination of the thermal conductivity of small
solids.
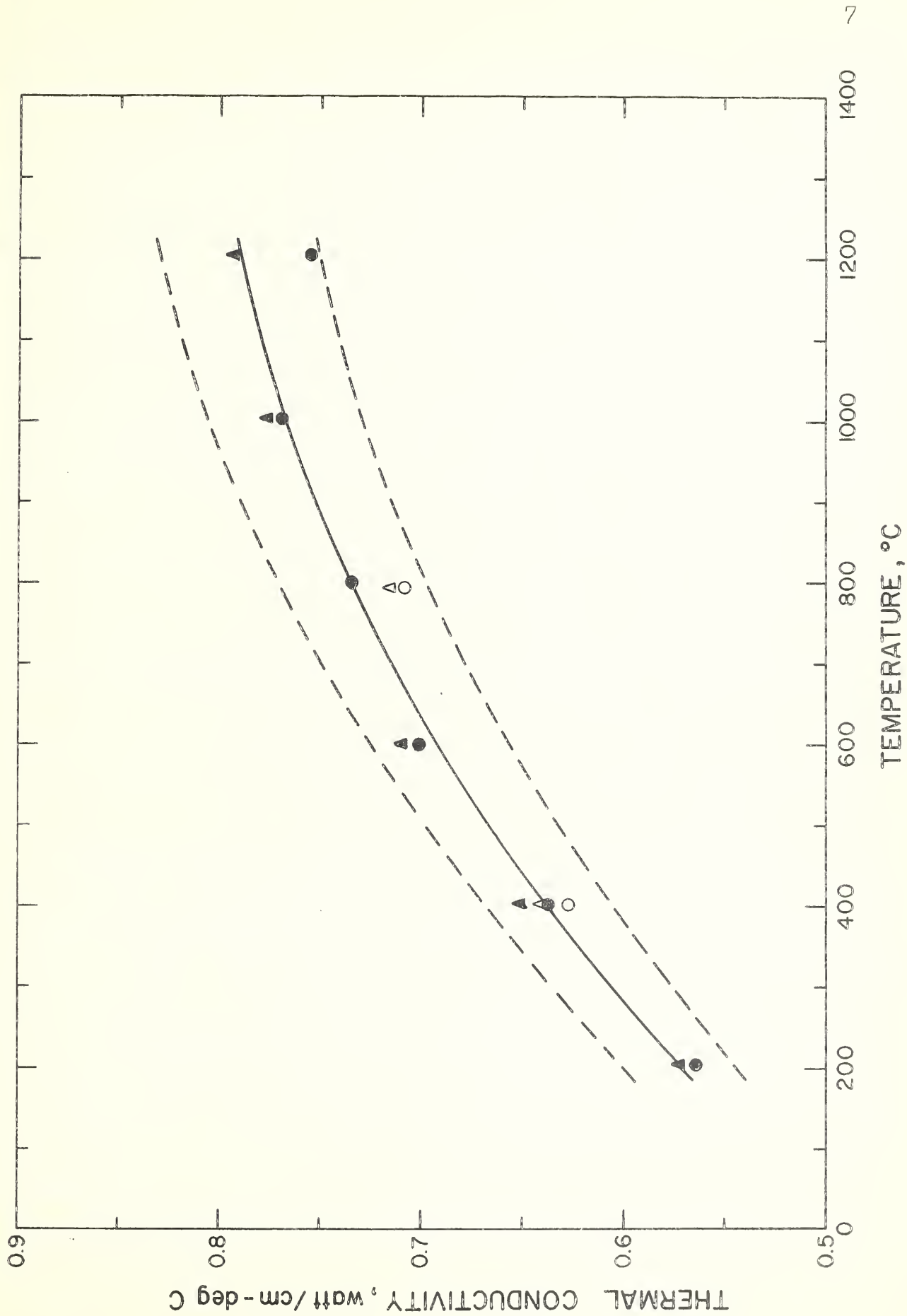
Figure 2. Tentative data for the thermal conductivity of a 60% platinum-40% rhodium alloy. The symbols are explained in the text.

THERMAL GUARDING OF CUT-BAR APPARATUS

D. R. Flynn*
National Bureau of Standards
Washington, D. C.

ABSTRACT

A mathematical analysis of heat transfer in the insulation sur-
rounding "cut-bar" thermal conductivity apparatus is presented. A general
solution is derived for arbitrary temperature distributions along the inner
and outer boundaries of the hollow cylinder of insulation.

For small heat exchanges between the insulation and metering bars
and specimen, the temperature distribution at the inner boundary is
approximated by three straight lines. Where temperature distribution along
the guard matches that along the meter bars and specimen, the heat gains or
losses to the insulation are proportional to:

1) The thermal conductivity of the insulation,

2) The difference between the thermal resistivities of the
specimen and meter bar,

3) A geometrical factor.

The choice of a meter bar becomes critical for low specimen con-
ductivities. Several conclusions are reached concerning the design and
operation of a cut-bar apparatus.

1. INTRODUCTION

The thermal conductivity of solid materials is of considerable
theoretical and practical interest. Unfortunately, published results for
this property are often widely divergent. While some variation among
literature data may be attributed to differences in sample composition and
mechanical properties, it is evident from the magnitude of these dis-
crepancies that errors exist in the various methods of measurement. These
errors can frequently be attributed to unaccounted for heat losses or gains
in a measuring apparatus.

One common method of determining thermal conductivity involves
the comparison of an unknown material with one of known conductivity. In
the comparative method, as usually employed, a sample of the unknown
material is placed in series with one or more samples of a known material
and a heat flow is established through this tandem assembly. A determina-
tion of the temperature gradient in the known material serves to define the
heat flow through the unknown sample.

A special case of the comparative method, sometimes designated as
the "cut-bar" method, has been used extensively and is the subject of this
paper. An unknown specimen is placed between two identical bars of a
"known" material, which, in actuality, serve as heat flow meters. (This
composite assembly, consisting of three bars in series will hereafter be

---

referred to as "the assembly.") The contacting surfaces of the meter bars and of the specimen are made flat and parallel, and a thrust is exerted on the assembly to assist good thermal contact. A temperature difference is maintained between opposite ends of the assembly, causing a heat flow along the bars and specimen. Thermocouples are employed to determine temperatures in the meter bars and specimen.

If data acquired by the cut-bar method are to be valid, care must be taken to minimize and account for heat gains or losses from the curved surfaces of the assembly. In this paper, analytical techniques are presented which assist in reducing and determining the magnitude of unwanted heat exchanges in the cut-bar method.

In order to minimize these heat exchanges, it is customary to provide a guard cylinder coaxial with the assembly, the space between the assembly and the guard cylinder being filled with thermal insulation. Usually, an attempt is made to maintain the same temperature distribution along the guard cylinder as along the assembly, so that guard temperatures match those of the assembly at corresponding longitudinal positions. This paper shows that this guarding technique does not preclude unwanted heat exchanges, and provides a means of computing and correcting for these exchanges.

2. MATHEMATICAL ANALYSIS

Figure 1 is a schematic of the assembly and surrounding insulation. For simplicity in the mathematical development, the meter bars are assumed to be identical in length and thermal conductivity.

K_m, K_S, and K_i are the thermal conductivities of the meter bars, the specimen, and the insulation, respectively. The radius, r, of the assembly is A; the inner radius of the guard is B; and the length of each reference bar is M; that of the specimen is L; and the over-all length is W=2M+L.

2.1 General Case

Consider the region consisting of the powder insulation between the assembly and the guard cylinder. The boundary conditions for this region can be expressed as:

1. $r=A$ $\quad 0 \le z \le W$ $\quad v=G(z)$

2. $r=B$ $\quad 0 \le z \le W$ $\quad v=H(z)$

3. $A \le r \le B$ $\quad z=0$ $\quad v=H(0)+\{G(0)-H(0)\}\frac{\ln B/r}{\ln B/A}$

4. $A \le r \le B$ $\quad z=W$ $\quad v=H(W)+\{G(W)-H(W)\}\frac{\ln B/r}{\ln B/A}$

(1)

where temperature is denoted by the symbol, v. G(z) and H(z) are the temperature distributions along the boundaries r=A and r=B, respectively. It has been assumed that the radial temperature distribution at the ends of the insulation, z=0 and z=W, can be represented logarithmically.

It is helpful to reduce all previously defined quantities to dimensionless forms:

$$\mu = z/W \quad ; \quad m = M/W \quad , \quad \ell = L/W$$

$$\rho = r/W \quad ; \quad a = A/W \quad , \quad b = B/W$$

$$\theta = (v - G(W))/T, \text{ where } T \equiv G(0)$$

$$\sigma_s = K_s/K_m \quad , \quad \sigma_i = K_i/K_m \quad . \tag{2}$$

In these reduced variables, the boundary conditions become

1.) $\rho = a$ $0 \leq \mu \leq 1$ $\theta = g(\mu)$

2.) $\rho = b$ $0 \leq \mu \leq 1$ $\theta = h(\mu)$

3.) $a \leq \rho \leq b$ $\mu = 0$ $\theta = 1 + \{h(0) - 1\}\dfrac{\ln \rho/a}{\ln b/a}$

4.) $a \leq \rho \leq b$ $\mu = 1$ $\theta = h(1)\dfrac{\ln \rho/a}{\ln b/a}$
$$\tag{3}$$

where all dimensionless temperatures, θ, have been referenced to $g(1) \equiv 0$, $g(0) \equiv 1$.

The heat flow in the hollow cylinder, $a \leq \rho \leq b$, must satisfy Laplace's equation in cylindrical coordinates, which in dimensionless parameters is, assuming angular symmetry

$$\frac{\partial^2 \theta}{\partial \rho^2} + \frac{1}{\rho}\frac{\partial \theta}{\partial \rho} + \frac{\partial^2 \theta}{\partial \mu^2} = 0 \quad . \tag{4}$$

Assume as a solution[1]*

$$\theta = \left[1 + \{h(0) - 1\}\frac{\ln \rho/a}{\ln b/a}\right](1-\mu) + h(1)\frac{\ln \rho/a}{\ln b/a} + \sum_{n=1}^{\infty} f_n(\rho)\sin n\pi\mu \tag{5}$$

in which

$$f_n(\rho) \equiv C_n I_0(n\pi\rho) + E_n K_0(n\pi\rho) \quad . \tag{6}$$

The boundary conditions (3) and (4) are satisfied by Equation (5). I_0 and K_0 are the zero order modified Bessel functions of the first and second kind, respectively.[2]

If $f_n(a)$ and $f_n(b)$ are the coefficients of the Fourier sine series at $\rho = a$ and $\rho = b$, respectively, then

$$C_n = \frac{f_n(a)K_0(n\pi b) - f_n(b)K_0(n\pi a)}{F_0(n\pi a; n\pi b)}$$

and

$$E_n = \frac{f_n(b)I_0(n\pi a) - f_n(a)I_0(n\pi b)}{F_0(n\pi a; n\pi b)} \quad , \tag{7}$$

where

$$F_0(x; y) \equiv I_0(x)K_0(y) - I_0(y)K_0(x), \tag{8}$$

and Equation (6) becomes

$$f_n(\rho) = \frac{f_n(a)F_0(n\pi\rho; n\pi b) - f_n(b)F_0(n\pi\rho; n\pi a)}{F_0(n\pi a; n\pi b)} \quad . \tag{9}$$

Boundary conditions (1) and (2) are satisfied if

$$f_n(a) = 2\int_0^1 \{g(\mu) - 1 + \mu\}\sin n\pi\mu \, d\mu \tag{10}$$

and

$$f_n(b) = 2\int_0^1 [h(\mu) - h(0) + \{h(0) - h(1)\}\mu]\sin n\pi\mu \, d\mu \tag{11}$$

---

* References appear under the heading REFERENCES.

Since the heat flux crossing the surface $\rho = a$ is of interest, Equation (5) is differentiated with respect to ρ, and evaluated at $\rho = a$:

$$(\frac{\partial\theta}{\partial\rho})_{\rho=a} = \frac{\{h(0)-1\}(1-\mu)+h(1)\mu}{a\ln b/a} + \sum_{n=1}^{\infty} n\pi f_n'(a)\sin n\pi\mu \tag{12}$$

where
$$f_n'(\rho) = \frac{f_n(a)F_1(n\pi\rho;n\pi b)-f_n(b)F_1(n\pi\rho;n\pi a)}{F_0(n\pi a;n\pi b)} \tag{13}$$

and
$$F_1(x;y) \equiv I_1(x)K_0(y)+I_0(y)K_1(x) \quad . \tag{14}$$

The radial flow of heat at the surface, $r=A$, through a cylindrical element of length dz is

$$dP = 2\pi A\ K_i(\frac{\partial v}{\partial r})_{r=a}dz \tag{15}$$

In the dimensionless parameters, this becomes

$$dp = 2\pi a\sigma_i(\frac{\partial\theta}{\partial\rho})_{\rho=a}d\mu \tag{16}$$

where $dp=dP/(WTK_m)$.

The total dimensionless power flowing across the surface $\rho=a$ between $\mu=0$ and $\mu=\mu_1$, where μ_1 is any arbitrary value $(0<\mu_1\leq 1)$, is

$$p(\mu_1) = 2\pi a\sigma_i\int_0^{\mu_1}(\frac{\partial\theta}{\partial\rho})_{\rho=a}d\mu \tag{17}$$

$$p(\mu_1) = 2\pi a\sigma_i\left[\frac{2\{h(0)-1\}\mu_1+\{1+h(1)-h(0)\}\mu_1^2}{2a\ln b/a} + \sum_{n=1}^{\infty}f_n'(a)(1-\cos n\pi\mu_1)\right] \tag{18}$$

Equation (18) is valid for any temperature distribution, $g(\mu)$, at $\rho=a$ and any temperature distribution, $h(\mu)$, at $\rho=b$. It will now be of interest to select a particular temperature distribution along the curved surface of the assembly, $\rho=a$.

2.2 Idealized Temperature Distribution on Inner Boundary

Returning to the apparatus of Figure 1, $f_n(a)$ will be evaluated for a particular choice of $g(\mu)$ (see Equation (10)). If the region $A\leq r\leq B$ contains a good insulation, the longitudinal temperature distribution at $r=A$ will approximate that which would exist in the absence of heat gains or losses. If S_m denotes the constant longitudinal temperature gradient in the meter bars and S_s that in the specimen (in the absence of any heat gains or losses), the temperature distribution, $G(z)$, at $r=A$ is

$$
\begin{array}{ll}
0\leq z\leq M & v=T-S_m z \\
M\leq z\leq M+L & v=T-S_m M-S_s(z-M) \\
M+L\leq z\leq W & v=T-S_m M-S_s L-S_m(z-M-L)=S_m(W-z)
\end{array}
\tag{19}
$$

The dimensionless temperature distribution, $g(\mu)$, at $\rho=a$ is

$$
\begin{array}{ll}
0\leq\mu\leq m & \theta=1-\psi_m\mu \\
m\leq\mu\leq m+l & \theta=1-\psi_m m-\psi_s(\mu-m) \\
m+l\leq\mu\leq 1 & \theta=\psi_m(1-\mu)
\end{array}
\tag{20}
$$

where
$$\psi_m = \frac{S_m W}{T}, \psi_s = \frac{S_s W}{T}$$

Substituting $g(\mu)$ from Equation (20) into Equation (10) and performing the indicated integration,

$$f_n(a) = \frac{4(\psi_m - \psi_s)}{n^2 \pi^2} \cos\frac{n\pi}{2} \sin\frac{n\pi\ell}{2} \quad . \tag{21}$$

It will now be helpful to eliminate ψ_m and ψ_s from Equation (21). If Q represents the total power that would be flowing longitudinally through the assembly if there were no heat gain or loss, then

$$Q = \pi A^2 K_m S_m = \pi A^2 K_s S_s \quad , \tag{22}$$

where πA^2 is the cross-sectional area of the assembly. In dimensionless parameters, this becomes

$$q = \frac{Q}{WTK_m} = \pi a^2 \psi_m = \pi a^2 \sigma_s \psi_s \quad . \tag{23}$$

Since $\psi_m = \sigma_s \psi_s$, $2m + \ell = 1$, and $2\psi_m m + \psi_s \ell = 1$, then

$$\psi_m = \frac{\sigma_s}{\sigma_s + (1 - \sigma_s)\ell} \text{ and } \psi_s = \frac{1}{\sigma_s + (1 - \sigma_s)\ell} \quad , \tag{24}$$

which can be substituted into Equations (21) and (23).

It is of interest to investigate the net fraction of power lost or gained between $\mu = 0$ and $\mu = \mu_1$.

$$\gamma(\mu_1) = \frac{p(\mu_1)}{q} \tag{25}$$

2.3 Matched Guarding

Since it is customary in thermal conductivity measurements to match the guard temperature distribution to that along the assembly, the first case to be studied will be that of a guard exactly matched in this respect. If the guard temperature distribution, $H(z)$, is identically equal to that along the bars and specimen, $G(z)$, the following equalities hold:

$$h(\mu) = g(\mu) \quad , \quad f_n(b) = f_n(a) \quad ,$$

and Equation (5) becomes

$$\theta = 1 - \mu + \sum_{n=1}^{\infty} f_n(\rho) \sin n\pi\mu \tag{26}$$

where now

$$f_n(\rho) = f_n(a)\frac{F_0(n\pi\rho; n\pi b) - F_0(n\pi\rho; n\pi a)}{F_0(n\pi a; n\pi b)} \quad . \tag{27}$$

From Equation (25), the net fraction of power lost or gained between $\mu = 0$ and $\mu = \mu_1$ becomes

$$\gamma(\mu_1) = \sigma_3(1 - \frac{1}{\sigma_2})D(\mu_1) = K_1(\frac{1}{K_m} - \frac{1}{K_s})D(\mu_1) \tag{28}$$

where
$$D(\mu_1) = \frac{2}{\pi^2 a} \sum_{n=1}^{\infty} U_n' (1 - \cos 2n\pi\mu_1) \tag{29}$$

and
$$U_n' = \frac{(-1)^n}{n^2} \left\{ \frac{F_1(2n\pi a; 2n\pi b) - 1/2n\pi a}{F_0(2n\pi a; 2n\pi b)} \right\} \sin n\pi\ell \tag{30}$$

since $F_1(x;x) \equiv 1/x$. Also, since $\cos n\pi/2 = 0$ for odd values of n, n has been replaced by 2n wherever it appears.

2.4 Unmatched Guarding

Any type of guarding desired can be studied by evaluating $f_n(b)$ in Equation (11) for an arbitrary guard temperature distribution, H(z). However, in this paper attention will be confined to cases of matched guarding.

3. NUMERICAL EXAMPLES FOR MATCHED GUARDING

The quantity of most interest in the above development is $\gamma(\mu_i)$ (Equations (25) and (28)), which is the net fraction of power lost to or gained from the insulation between $\mu = 0$ and $\mu = \mu_1$.

Since $D(\mu_1)$ in Equation (28) is a function of dimensionless geometric parameters only, it represents a geometrical factor which depends only on the shape of the particular apparatus being considered. . For a given geometry, the fractional parasitic heat flow is proportional to the thermal conductivity of the surrounding insulation and to the difference of the reciprocal thermal conductivities (resistivities) of the meter bars and specimen.

A schematic diagram of a particular cut-bar apparatus is shown in the upper left-hand corner of Figure 2. The meter bars and specimen are equal in length; this length is equal to twice their diameter. The radius of the guard has been chosed as 1.5 times that of the bars. For numerical evaluation, the specimen and insulation have been chosen to have, respectively, thermal conductivities 1/5 and 1/100 that of the meter bars.

The graph in the lower left-hand corner of Figure 2 illustrates the dimensionless longitudinal temperature distribution that would exist along the meter bars and specimen in the absence of heat exchanges with the insulation. The vertical dashed lines indicate the positions of the interfaces between the meter bars and the specimen. Since, in this case, an exactly matched guard is being considered, the temperature distribution shown is also that which exists along the guard.

The graph in the upper right-hand corner of Figure 2 illustrates the dimensionless radial temperature gradient which exists in the insulation at the convex surface of the meter bars and specimen. The quantity shown, which is plotted against dimensionless length, is $(\partial\theta/\partial\rho)_{\rho=a}$ from Equation (12), where appropriate substitutions have been made corresponding to the case of matched guarding. In this particular case, the radial gradient is substantially zero, except in the regions near the interfaces. In this graph, the peaks at the interfaces have arbitrarily been cut off at -1.0 and +1.0.

The effect of such a radial gradient distribution is shown in the graph in the lower right-hand corner of Figure 2. The fractional power change $\gamma(\mu_1)$, from Equation (28), is plotted versus dimensionless length. The quantity plotted is actually $100\gamma(\mu_1)$, which expresses the percentage change of power flowing longitudinally through the meter bars and specimen.

In this graph, the power flowing in the first meter bar is seen to remain constant until the interface is approached. The power drops rapidly near the interface, then levels off in the specimen to a constant value approximately 2.2 percent less than that which was flowing in the first meter bar. Near the second interface, the longitudinal heat flow increases so that its rate is the same in the second meter bar as it was in the first.

3.1 Influence of Thermal Conductivity

It was seen in Equation (28) that, for matched guarding

$$\Upsilon(\mu_1) = K_i(\frac{1}{K_m} - \frac{1}{K_S})D(\mu) \tag{28}$$

where $D(\mu)$ is a geometrical factor. To illustrate the errors that would arise if a range of materials were measured using the same meter bar and insulation, the fractional power change is plotted in Figure 3 versus dimensionless length for a variety of specimen thermal conductivities. The geometry of the apparatus and the ratio of the thermal conductivity of the insulation to that of the meter bars are the same as in Figure 2. The quantity $100\Upsilon(\mu_1)$ is shown for specimens having a thermal conductivity ranging from one-tenth to ten times that of the meters.

The effect of varying specimen thermal conductivity for different meter bars is shown in greater detail in Figure 4. Here the coefficient conductivity-term of Equation (28)

$$K_i(\frac{1}{K_m} - \frac{1}{K_S})$$

is plotted against K_S, the thermal conductivity of the specimen, for four values of K_m, the thermal conductivity of the meter bars. The thermal conductivity of the insulation is held fixed at 0.001 w/cm-C. The quantity plotted goes through zero at $K_S = K_m$, approaches $-\infty$ as K_S becomes quite small, and asymptotically approaches K_i/K_m as K_S becomes large.

As will be illustrated later, a typical geometrical factor, $D(\mu)$, would probably not exceed a value of 2.5. If the vertical scale in Figure 4 were multiplied by 2.5, each scale division, 0.02, would become 0.05, or 5 percent. Hopefully, the geometrical factor might be made as small as 0.5, or 1.0, so that each vertical scale division would become 1 or 2 percent, respectively.

If both the specimen and the meter bars have at least one hundred times the thermal conductivity of the insulation, the choice of a particular meter bar is not critical. If the specimen to be measured has a thermal conductivity on the order of ten times that of the insulation, or less, the choice of a suitable meter bar becomes quite important.

It can be seen from Figure 4 that the conductivity of the meter bars should be near the lower end of the range to be covered, if it is desired to measure a wide range of specimen thermal conductivities, utilizing a single pair of meter bars. If

$$K_m = \frac{2(K_S)_{max} (K_S)_{min}}{(K_S)_{max} + (K_S)_{min}} \tag{31}$$

where $(K_S)_{max}$ and $(K_S)_{min}$ are the maximum and minimum specimen thermal conductivities to be measured, then the maximum error to be expected within the range is

$$\pm \frac{K_i}{2}(\frac{1}{(K_S)_{max}} - \frac{1}{(K_S)_{min}})D(\mu) \tag{32}$$

For relatively large $(K_s)_{max}$, Equation (31) reduces to

$$K_m \approx 2(K_s)_{min} \tag{33}$$

and the maximum error over the range (Equation (32)) becomes

$$\pm \frac{1}{2} \frac{K_i}{(K_s)_{min}} D(\mu) \tag{34}$$

It is of interest to investigate numerically the significances of Equations (31) and (32). Table 1 gives several ranges of thermal conductivity, the preferred meter bar for each range, and the maximum error to be expected for a given geometrical factor (1.0) and insulation thermal conductivity (0.001 w/cm-C).

TABLE 1. MAXIMUM ERROR FOR VARIOUS RANGES OF SPECIMEN THERMAL CONDUCTIVITY

K_s			Maximum Error
Minimum	Maximum	Optimal K_m	in K_s Range
w/cm-C	w/cm-C	w/cm-C	± %
0.005	0.01	0.0067	5.0
.01	.015	.0120	1.7
.01	.02	.0133	2.5
.01	.05	.0167	4.0
.01	.10	.0182	4.5
.01	1.00	.0198	5.0
.05	.10	.0667	.50
.05	.50	.0909	.90
.10	.50	.167	.40
.10	1.00	.182	.45
.10	10.00	.198	.50
1.00	10.00	1.82	.045

3.2 Geometrical Factor

Returning to Equation (28), it is of interest to investigate the behavior of the geometrical factor $D(\mu)$. The numerical evaluation of $D(\mu)$ from Equation (29) has been made with the use of a digital computer, and required summing the first hundred terms of the series in order to obtain sufficient accuracy.

Figure 5 shows the geometrical factor, $D(\mu)$, plotted versus μ, the dimensionless length. The geometry chosen is such that the meter bars and specimen are of equal length. The radius of the guard is taken as 1.5 times that of the bars'. The geometrical factor is shown for five values of $L/2A$, the ratio of specimen length to specimen diameter. Due to the boundary conditions imposed, $D(\mu)$ is zero at $\mu=0$ and $\mu=1$, regardless of the particular geometry. Since these geometrical factors are symmetrical about the center line of the specimen, they are not shown for μ greater than 0.5.

For the case of $L/2A=0.2$, a stack of disks each only 1/5 as thick as it is across, the geometrical factor is changing over the entire length of the meter bars and specimen; there is no substantial region where the longitudinal heat flow is constant. Similarly, there is no substantial region within the meter bars and specimen free of radial temperature gradients.

For the case of L/2A=0.5, the geometrical factor at the center of the specimen is significantly larger than that for L/2A=0.2. However, as L/2A increases further, the geometrical factor near the center of the specimen approaches a limiting value of about 0.54.

As the ratio of specimen length to specimen diameter, L/2A, increases, the fraction of the specimen length over which $D(\mu)$ is substantially constant also becomes larger. Similarly, the fraction of the meter bars over which $D(\mu)$ is substantially zero becomes larger. To illustrate this effect, a somewhat arbitrary criterion has been chosen.

Consider the dashed curve superimposed on Figure 5. The portion of each $D(\mu)$ curve above the point at which the dashed line intersects a $D(\mu)$ curve is within 5 percent of the peak value of that curve. This dashed curve and its mirror image (not illustrated here) bound the fraction, $\overline{L}/L$, of specimen length over which $D(\mu)$ is within 5 percent of $D(1/2)$.

In the insert in Figure 5, the fraction of specimen length, $\overline{L}/L$, bounded by the dashed curve and its mirror image, is plotted against the ratio, L/2A, of specimen length to specimen diameter. This graph indicates that only 41 percent of the specimen length satisfies the arbitrary flatness criterion for L/2A=0.2, while for L/2A=5.0, 93 percent of the specimen length satisfies the criterion.

Figure 6 is similar to Figure 5, except that the radius of the guard is taken as 3.0 times that of the bars. The vertical scale is five times as large as that in Figure 5. The curves shown do not reach their limiting value until L/2A=5.0 and even then, only 72 percent of the specimen satisfies the flatness criterion.

Figure 7 shows the geometrical factor plotted against dimensionless length for a specimen length to specimen diameter ratio fixed at 2.0. Curves are shown for guard to specimen radius ratios, B/A, ranging from 1.125 to 3.5. The geometrical factor at the center of the specimen increases rapidly with B/A. For small values of B/A, $\overline{L}/L$ is quite large, but decreases rapidly with increasing B/A, as shown on the inset.

As was noted in Figures 5 and 6, $D(\mu)$ reaches a limiting value for a fixed B/A as L/2A becomes quite large. This limiting value, $D(1/2)_{max}$, is shown plotted against B/A in Figure 8. Regardless of the apparatus geometry, $D(\mu)$ will never exceed $D(1/2)_{max}$ for a given guard to bar radius ratio.

Considerable insight into the nature of $D(1/2)_{max}$ can be gained by consideration of a simplified model. It has been shown that, for sufficiently long meter bars and specimen, the power flowing longitudinally in the meter bars is constant, until the interface with the specimen is approached, and that the power flowing in the central portion of the specimen is also constant, but at a different value. The portion of the insulation near the bar assembly will exchange heat only with the assembly; similarly, the remainder of the insulation will exchange heat only with the guard. The geometrical factor, $D(1/2)_{max}$, can be regarded as the ratio of the cross-sectional area of the insulation which exchanges heat only with the assembly, to the cross-sectional area of the bar assembly.

4. DISCUSSION

The error due to neglecting the longitudinally shunting effect of the insulation has been analyzed for a cut-bar apparatus having an exactly matched guard. For such a guard, longitudinal heat flow in the insulation can be minimized by making the radius of the guard very nearly that of the bar. In practice, an exactly matched guard is not feasible, so that

radial heat exchange between the assembly and guard due to a mismatch also must be considered.

Assume that the largest probable mismatch between corresponding longitudinal positions of the bars and guard is ε, a dimensionless temperature difference. The worst case would be that of the entire guard being displaced by an amount, ε, so that $h(\mu)=g(\mu)+\varepsilon$. In this case, Equation (11) is the same as Equation (10). Therefore, the radial heat flow between the assembly and the guard is independent of the shunting heat flow and, from Equation (18), the heat flow to the guard due to a uniform mismatch is seen to be given by the usual logarithmic expression. The error due to radial flow can be computed for various guard diameters and, by comparison with the error due to shunting heat flow, a guard can be selected so that the sum of these errors is approximately minimized.

An analysis similar to that presented in this paper is being used at NBS to correct for heat exchanges in the absolute cut-bar apparatus. The analysis has been very helpful in aiding our understanding of the problems involved, and is in fact regarded as essential in the effort to reduce uncertainties in the results obtained with the apparatus.

It is hoped that the analysis and discussion presented in this paper will be of assistance to those who are utilizing a cut-bar apparatus. It is realized that many laboratories will not find it convenient to resort to a digital computer for evaluation of their particular geometrical factors. Mr. Robinson pointed out the advantages of utilizing a substitution method for calibrating a thermal conductivity apparatus. By using several references as substitute specimens, the effect of shunting heat flows in the insulation can be included in the calibration, and the geometrical factor, if desired, can be experimentally evaluated.

REFERENCES

(1) Carslaw and Jaeger, <u>Conduction of Heat in Solids</u>, Second Edition, Oxford University Press (1959) pp 214-229

(2) Watson, <u>Theory of Bessel Functions</u>, Cambridge University Press (1944)
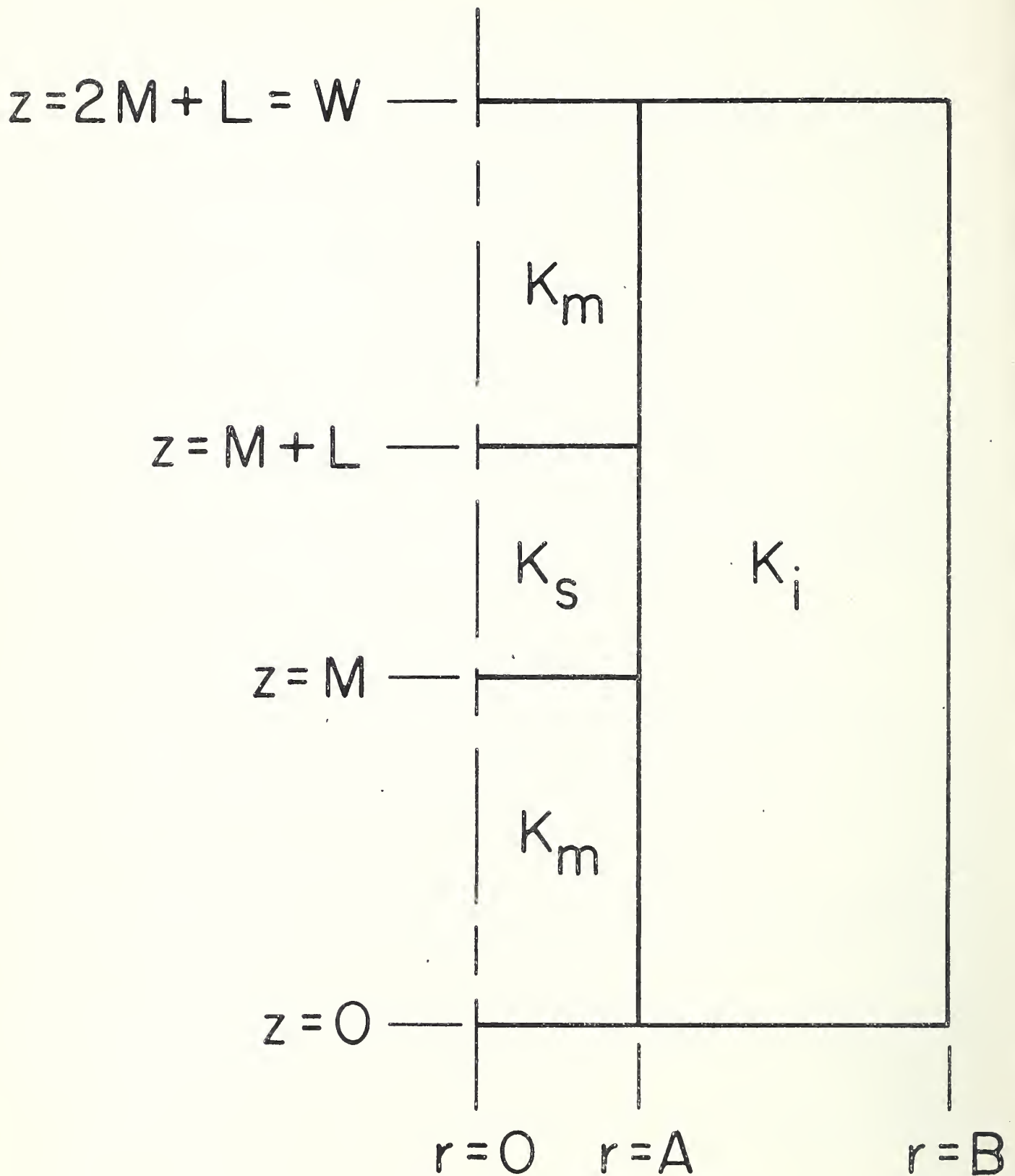
Figure 1. Schematic diagram of meter bars, specimen, and
surrounding insulation.
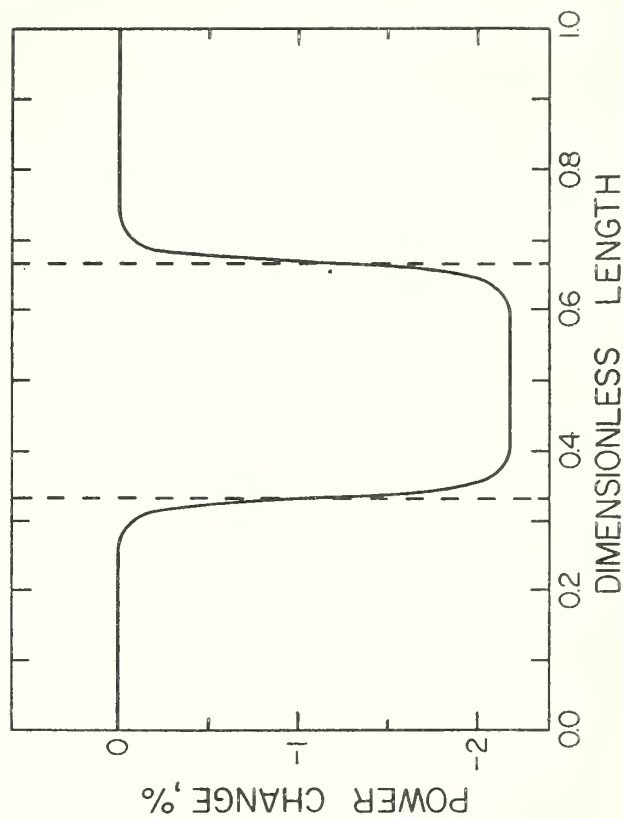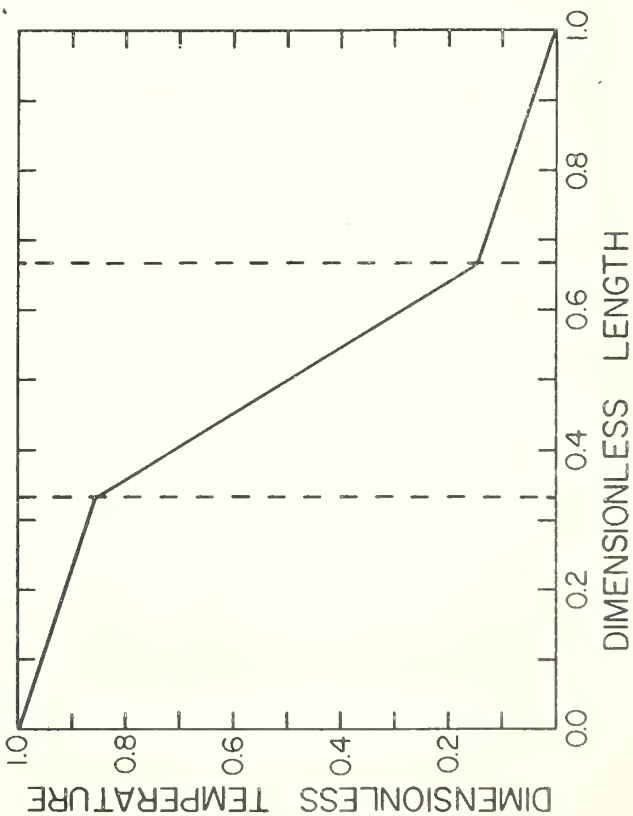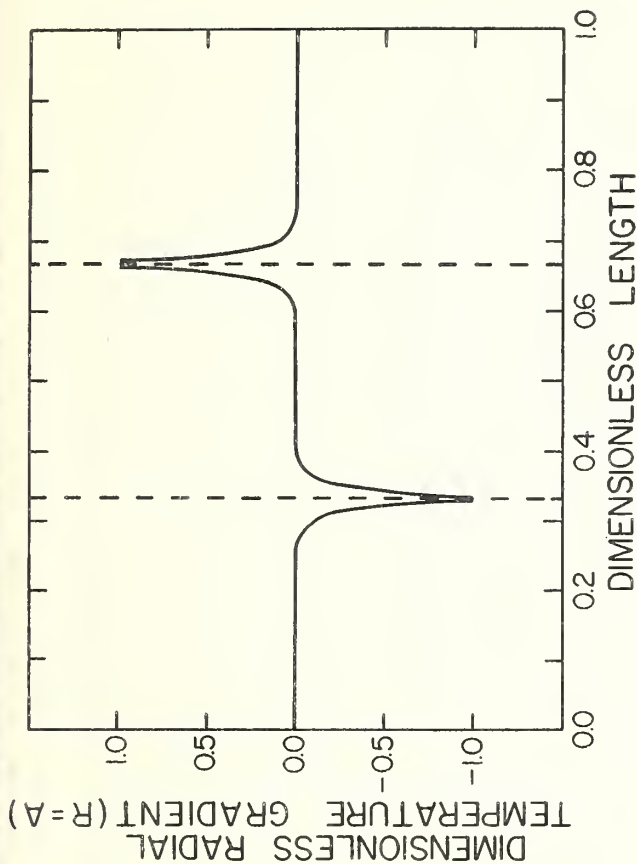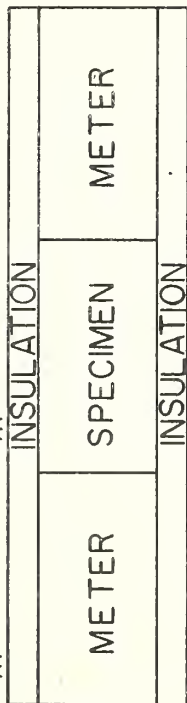
Figure 2. Dimensionless temperature distribution, dimensionless radial temperature gradient at surface of bars, and fractional change in power for a particular cut-bar apparatus.
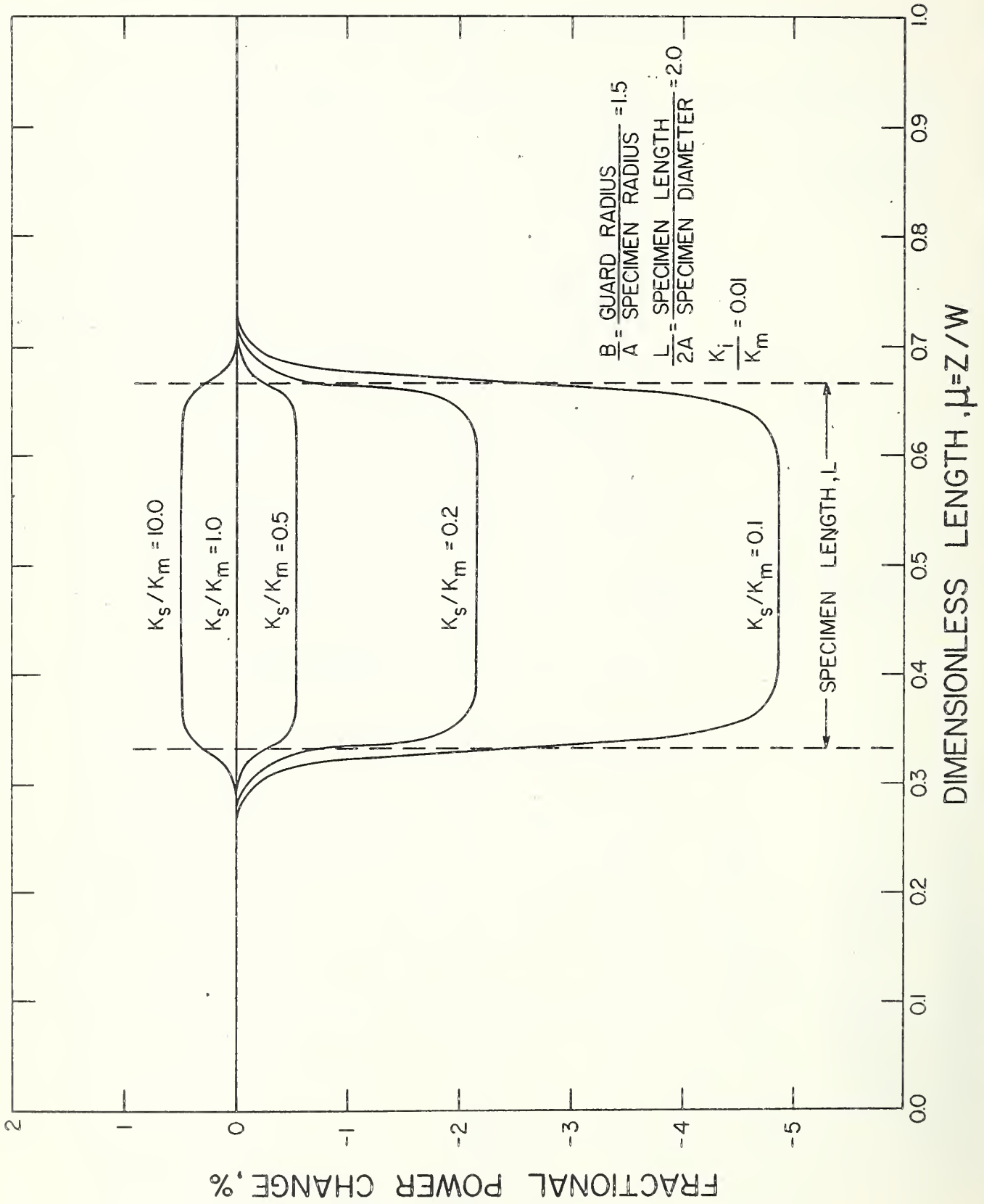
Figure 3. Fractional power change for a range of specimen thermal conductivities.
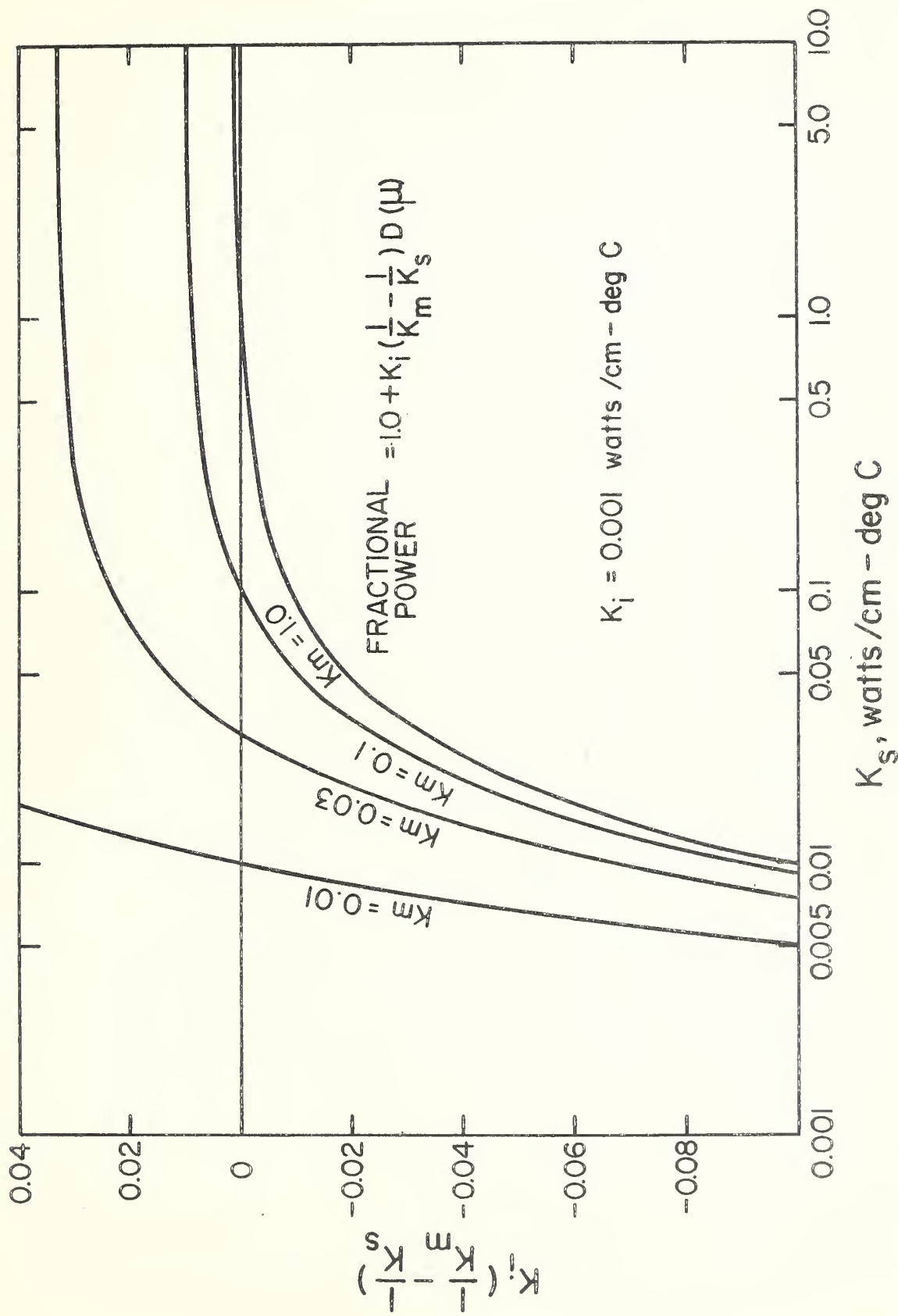
Figure 4. Effect of specimen thermal conductivity on the fractional power change for several meter bars.
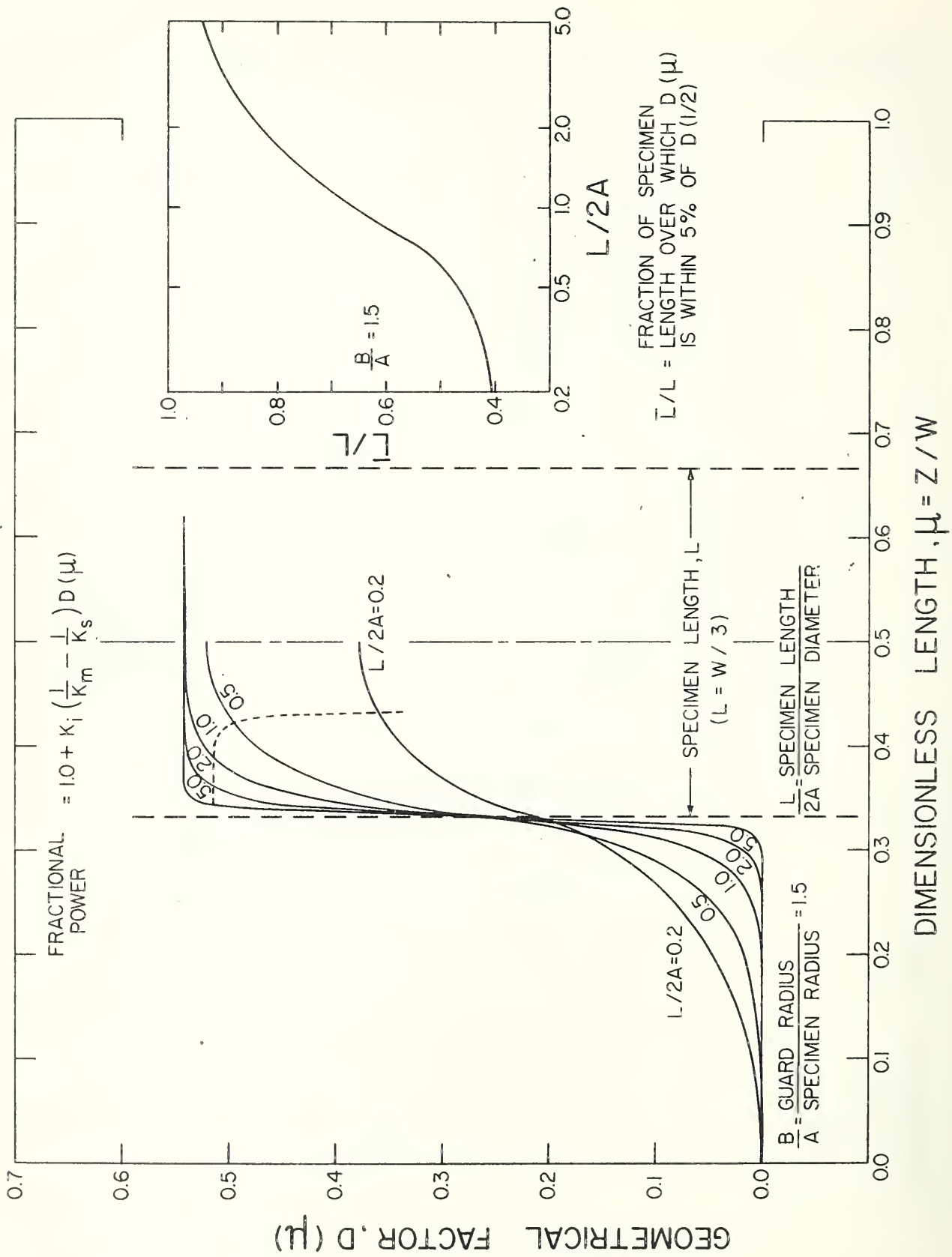
Figure 5. Geometrical factor for five ratios of specimen length to diameter, with the guard to bar radius ratio held at 1.5.
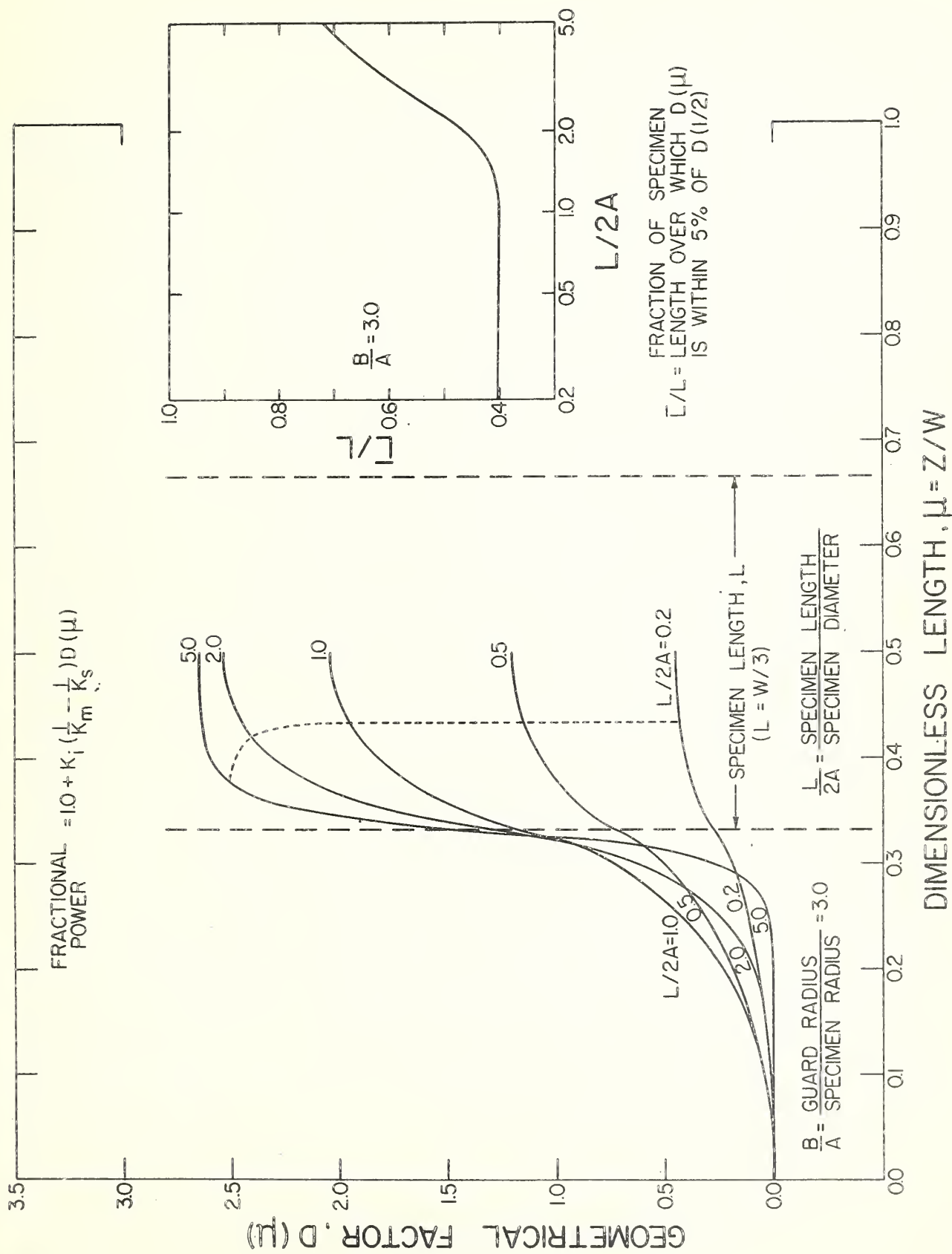
Figure 6. Geometrical factor for five ratios of specimen length to diameter, with the guard to bar radius ratio held at 3.0.
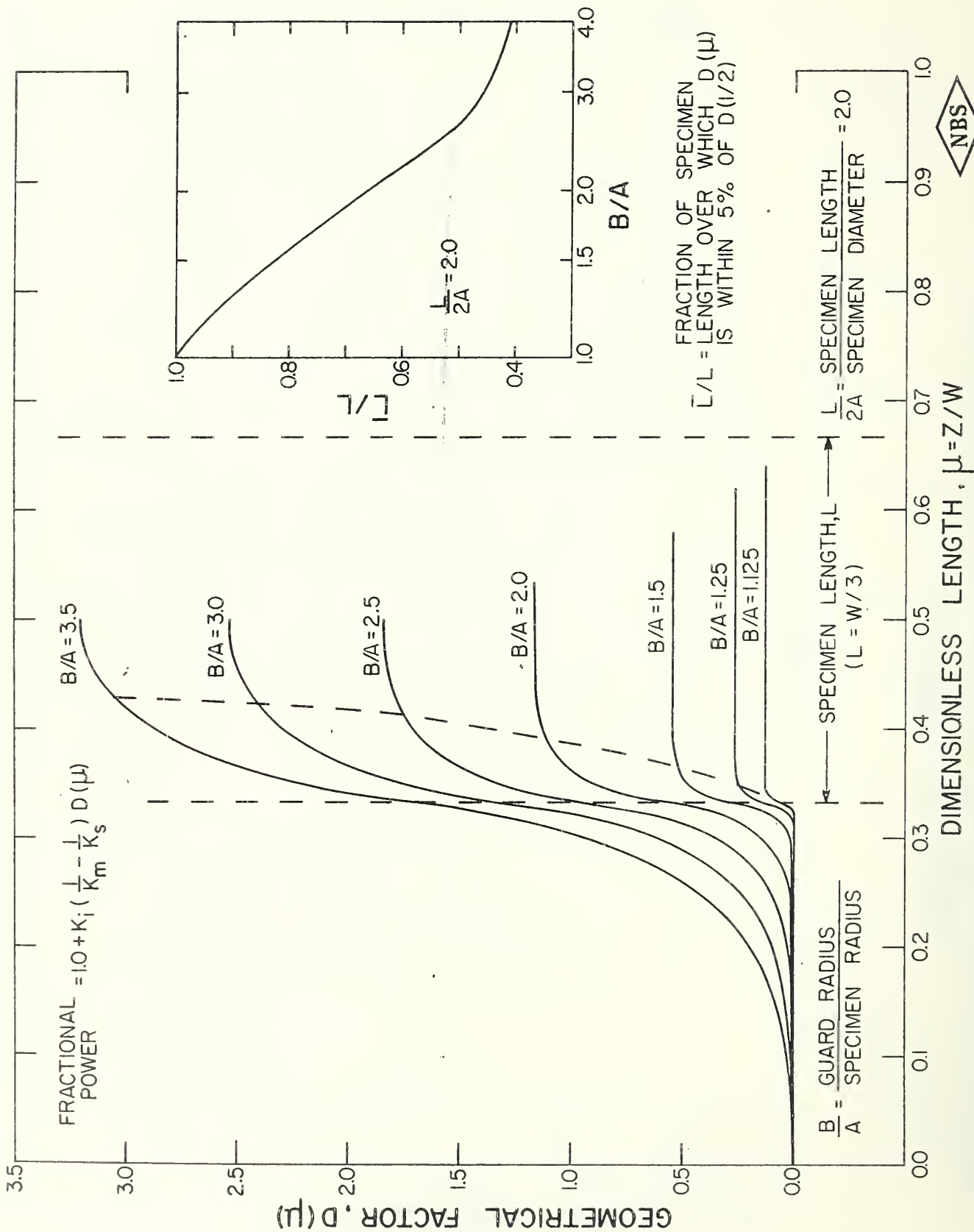
Figure 7. Geometrical factor for seven ratios of guard to bar radius, with the specimen length to diameter ratio held at 2.0.
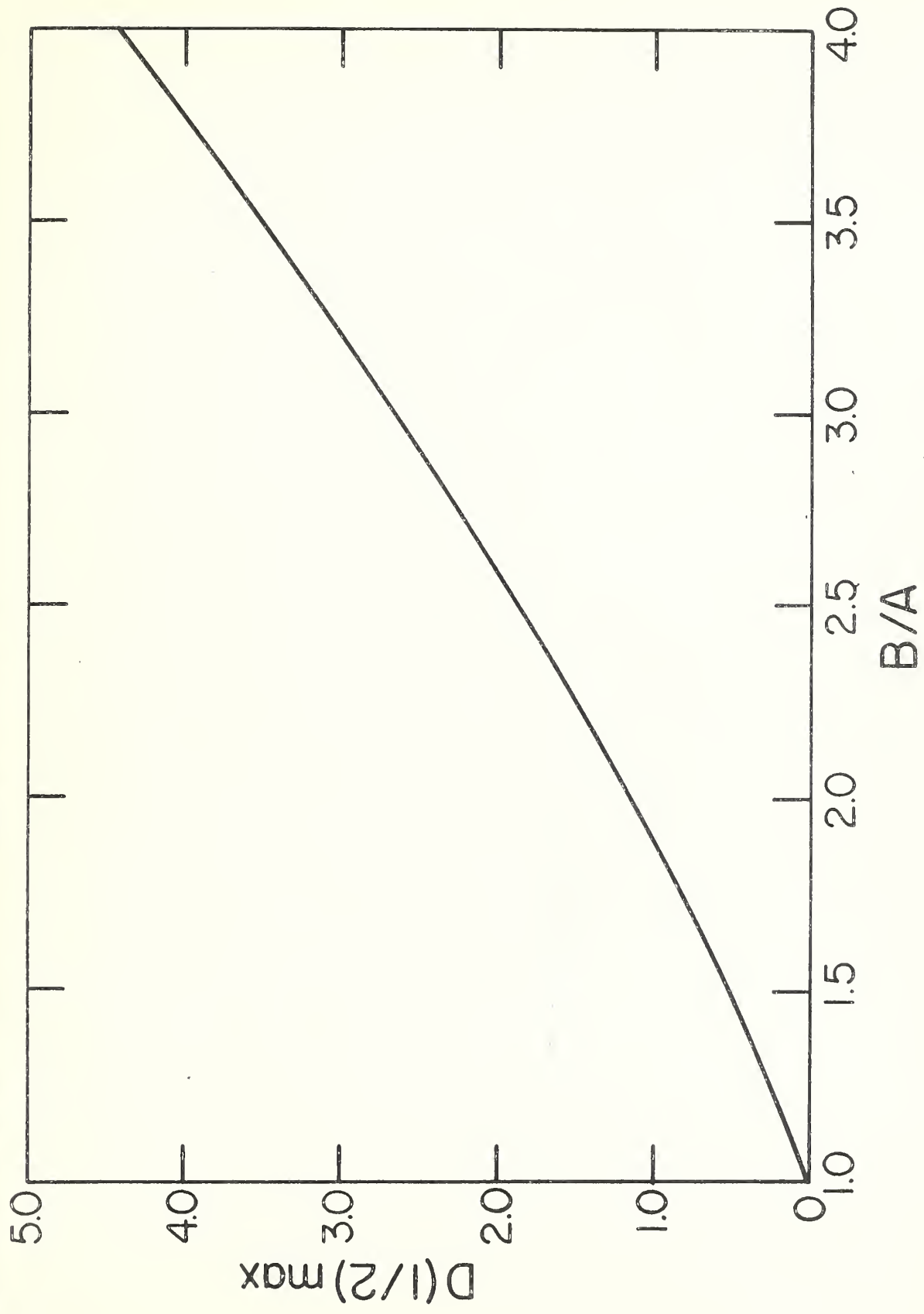
Figure 8. Maximum value of the geometrical factor as a function of the ratio of guard to bar radius.
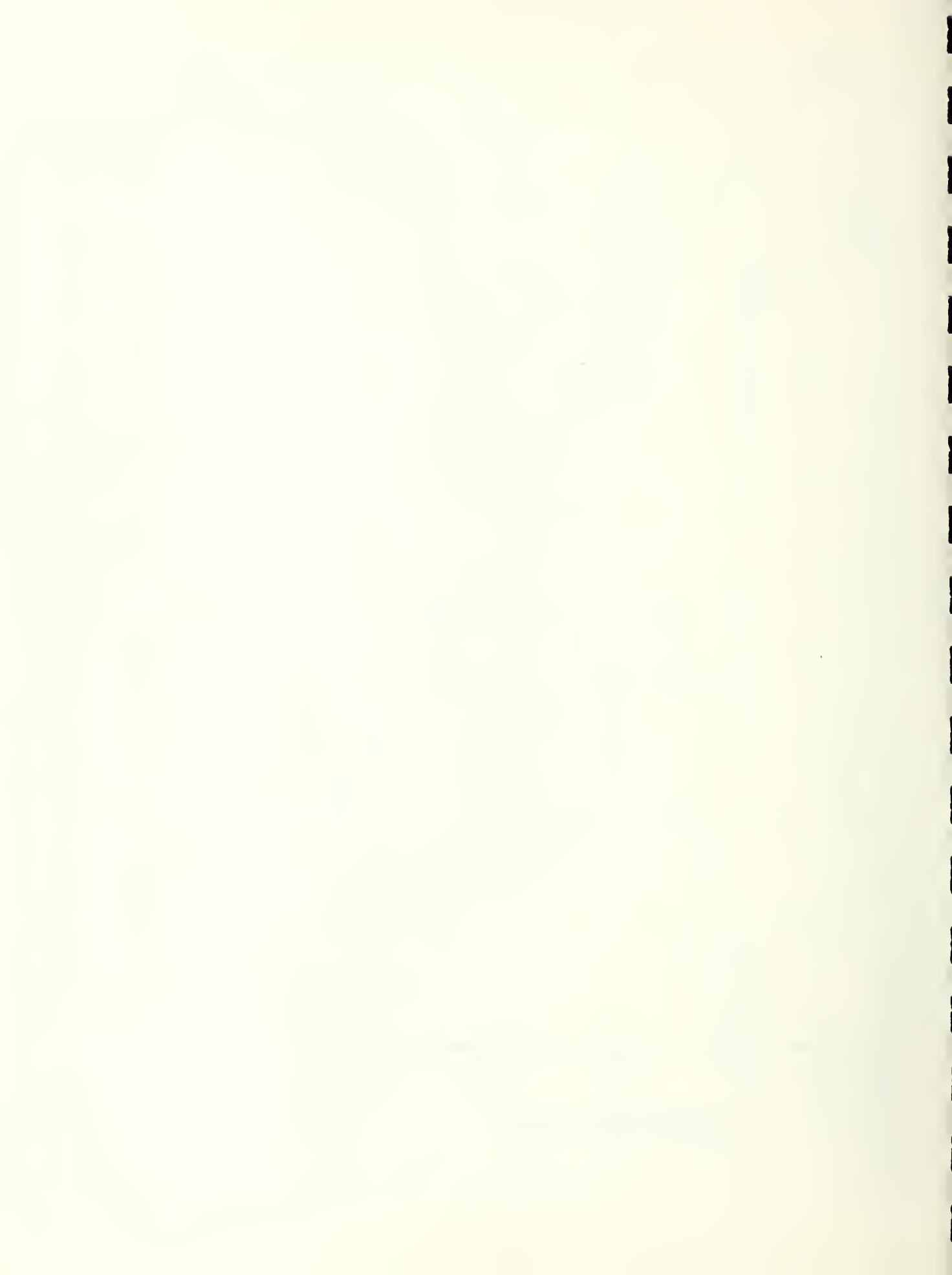
THE NATIONAL BUREAU OF STANDARDS

The scope of activities of the National Bureau of Standards at its major laboratories in Washington, D.C., and Boulder, Colorado, is suggested in the following listing of the divisions and sections engaged in technical work. In general, each section carries out specialized research, development, and engineering in the field indicated by its title. A brief description of the activities, and of the resultant publications, appears on the inside of the front cover.

WASHINGTON, D.C.

Electricity. Resistance and Reactance. Electrochemistry. Electrical Instruments. Magnetic Measurements. Dielectrics. ·

Metrology. Photometry and Colorimetry. Refractometry. Photographic Research. Length. Engineering Metrology. Mass and Scale. Volumetry and Densimetry.

Heat. Temperature Physics. Heat Measurements. Cryogenic Physics. Equation of State. Statistical Physics.

Radiation Physics. X-ray. Radioactivity. Radiation Theory. High Energy Radiation. Radiological Equipment. Nucleonic Instrumentation. Neutron Physics. ·

Analytical and Inorganic Chemistry. Pure Substances. Spectrochemistry. Solution Chemistry. Standard Reference Materials. Applied Analytical Research.

Mechanics. Sound. Pressure and Vacuum. Fluid Mechanics. Engineering Mechanics. Rheology. Combustion Controls.

Organic and Fibrous Materials. Rubber. Textiles. Paper. Leather. Testing and Specifications. Polymer Structure. Plastics. Dental Research.

Metallurgy. Thermal Metallurgy. Chemical Metallurgy. Mechanical Metallurgy. Corrosion. Metal Physics. Electrolysis and Metal Deposition.

Mineral Products. Engineering Ceramics. Glass. Refractories. Enameled Metals. Crystal Growth. Physical Properties. Constitution and Microstructure.

Building Research. Structural Engineering. Fire Research. Mechanical Systems. Organic Building Materials. Codes and Safety Standards. Heat Transfer. Inorganic Building Materials.

Applied Mathematics. Numerical Analysis. Computation. Statistical Engineering. Mathematical Physics. Operations Research.

Data Processing Systems. Components and Techniques. Digital Circuitry. Digital Systems. Analog Systems. Applications Engineering.

Atomic Physics. Spectroscopy. Infrared Spectroscopy. Solid State Physics. Electron Physics. Atomic Physics.

Instrumentation. Engineering Electronics. Electron Devices. Electronic Instrumentation. Mechanical Instruments. Basic Instrumentation.

Physical Chemistry. Thermochemistry. Surface Chemistry. Organic Chemistry. Molecular Spectroscopy. Molecular Kinetics. Mass Spectrometry.

Office of Weights and Measures.

BOULDER, COLO.

Cryogenic Engineering. Cryogenic Equipment. Cryogenic Processes. Properties of Materials. Cryogenic Technical Services.

Ionosphere Research and Propagation. Low Frequency and Very Low Frequency Research. Ionosphere Research. Prediction Services. Sun-Earth Relationships. Field Engineering. Radio Warning Services.

Radio Propagation Engineering. Data Reduction Instrumentation. Radio Noise. Tropospheric Measurements. Tropospheric Analysis. Propagation-Terrain Effects. Radio-Meteorology. Lower Atmosphere Physics.

Radio Standards. High Frequency Electrical Standards. Radio Broadcast Service. Radio and Microwave Materials. Atomic Frequency and Time Interval Standards. Electronic Calibration Center. Millimeter-Wave Research. Microwave Circuit Standards. ·

Radio Systems. High Frequency and Very High Frequency Research. Modulation Research. Antenna Research. Navigation Systems.

Upper Atmosphere and Space Physics. Upper Atmosphere and Plasma Physics. Ionosphere and Exosphere Scatter. Airglow and Aurora. Ionospheric Radio Astronomy.